Effect of eliminating the decaying direct current component from the current signal on the discrete fourier transform based phasor estimation technique

Hesham B. Elrefaie
Electrical Eng. Dept., Faculty of Eng., Alexandria University, P.O. Box 21544, Alexandria, Egypt

The technique suggested by Ferrero et al. for eliminating the decaying direct current component from the current signal has been used for identifying the fault type using a fuzzy set approach. To the knowledge of the author, this technique has never been used for studying the effect of eliminating the decaying direct current component from the current signal on the phasor estimation. This technique is used in this paper to study the effect of eliminating the decaying direct current component from the current signal on the discrete Fourier transform based phasor estimation technique. A comparative study has been carried out between the results obtained from this technique and other techniques published in literature for eliminating the direct current component and the phasor estimation. The Alternative Transient Program (ATP) is used to generate the voltage and current signals needed for estimating phasors and the Matlab software package is used to simulate the phasor estimation techniques. The results of the phasor estimation technique suggested by Ferrero et al. are more accurate and converged to the desired values faster than the other techniques published in refs .

استخدمت تقنية فيريرو لحذف مركبة التيار المستمر المضمحلة من اشارة التيار الكهربى فى تعريف أخطاء خطوط نقل القدرة الكهربية باستخدام مدخل الفئة المبهم ولم تستخدم من قبل فى دراسة تأثير حذف مركبة التيار المستمر المضمحلة من اشارة التيار الكهربى على استنتاج المتجة الدوار. استخدمت تقنية فيريرو فى هذه المقالة فى دراسة تأثير حذف مركبة التيار المستمر المضمحلة من اشارة التيار الكهربى على استننتاج المتجة الدوار باستخدام تحويل فورير المتقطع وتم عمل دراسة مقارنة بين نتائج هذة التقنية ونتائج تقنيات أخرى لحذف مركبة التيار المستمر المضمحلة واستخدم برنامج الحالات العابرة فى توليد موجات الجهد و ا لتيار المستخدمة فى حساب المتجة الدوار و استخدم برنامج ماتلاب لتمثيل تقنيات استنتاج المتجة الدوار. واستخلص من هذة الدراسة أن نتائج قيم المتجة الدوار المستنتجة بطريقة فريرو قريبة جدا الى القيم المطلوبة وتؤول بسرعة كبيرة الى هذة القيم مقارنة بالطرق الأخرى.

Keywords: Digital protection of power systems, Discrete fourier transform, Phasor estimation techniques, Decaying DC components, Alternative transient program, Matlab software package

1. Introduction

The Discrete Fourier Transform (DFT) [1] is the most commonly used algorithm in digital relaying devices in electrical power systems. In most cases, it is used to estimate the phasors of the fundamental frequency component, based on which the relays make necessary decisions. Although different data windows have been suggested, full cycle DFT (FCDFT) is the most widely used.

Decaying DC offsets are generated following any fault or disturbance in an electrical power system. The decay rates are dependent on the time constants determined by the X/R ratio (inductive reactance to resistance ratio) of the system. The larger the X/R ratio, the slower the direct current decays. A decaying DC offset is a non-periodic signal and has a relatively wide range frequency spectrum. The decaying DC affects the accuracy the of DFT algorithm results.

The analysis of the negative effects of the decaying DC on DFT phasor estimation has been reported by Benmouyal [2]. The error of the DFT phasor estimation can reach up to 15.1% according to [2]. The error due to the decaying DC offset in phasor measurement of the DFT is significant and can not be tolerated in most relay applications. Consequently, special measures should be taken to reduce or eliminate this negative effect.

A number of methods have been proposed to reduce or eliminate the negative effects of decaying DC components. In [2], a mimic filter plus DFT is proposed to filter out the decaying offset. Some performance indexes have also been suggested to evaluate the effectiveness of DC removal algorithms. The decaying DC offset can be totally removed when the time constant of the DC component matches with the one assumed in the mimic filter. However, this is not realistic because the time constant varies over a wide range depending on the system configuration and fault location. Fault resistance may make the range of deviation of the time constant even wider. The performance of this algorithm is tested in [2] when the time constant varies between 0.5 and five cycles. The time response of this algorithm shows that its estimation deteriorates when the time of the mimic filter is tuned at two cycles while the actual time constant is 0.5 cycles. When the variations of the time constant exceeds this range, the performance of the mimic filter may even further deteriorate. The mimic filter will also introduce an additional delay of one sample.

Yang and Liu [3] have proposed a DFT based algorithm to completely remove the decaying DC component. This algorithm uses three continuous DFT results to calculate the unknown parameters of the decaying DC component. Thus, the time constant and magnitude of the decaying DC component can be exactly obtained, and the decaying DC component can be removed.

Sidhu et al. [4] proposed a DFT-based filtering technique to remove the decaying DC component. This algorithm uses two FCDFT filters, one tuned at the fundamental frequency and the other at the m th harmonic. The purpose of the m th harmonic FCDFT is to determine the decaying DC parameters. Once the parameters of the decaying DC offset are found, the phasor corresponding to the decaying DC component is determined. The phasor corresponding to the fundamental frequency component can be extracted by taking the difference between the phasor corresponding to the total input signal (obtained from the output of fundamental frequency filter) and the phasor corresponding to the decaying DC parameters.

Shan [5] derived a mathematical expression for the error resulting from estimating a phasor with the DFT. The source of this error is the decaying DC component presented in the signal used in estimating the phasor. This error is a function of two sequential phasors estimated by the DFT algorithm. The accurate real and imaginary part of the fundamental phasor can be calculated from the error. He developed also an adaptive scheme to find the decaying DC time constant.

Guo et al. [6] used two partial sums to estimate the parameters of the decaying DC component presented in the current signal. The first is the sum of the odd number samples taken from a complete cycle of the current signal (corresponding to the fundamental frequency). The second is the sum of the even number samples taken from a complete cycle of the current signal. Once the parameters of the decaying DC component are obtained, a new set of sampled values can be extracted by taking the difference between the original sampled values (corrupted by the decaying DC component) and a set of sampled values representing the decaying DC component. This new set of sampled values no longer contains the exponentially decaying DC component. Applying the Fourier algorithm to this new set of samples, the phasor corresponding to the fundamental frequency component can be estimated.

The technique suggested by Ferrero et al. [7] is used in this paper to study the effect of eliminating the decaying DC component from the current signal on the DFT based phasor estimation. A comparative study has been carried out between the results obtained from this technique and the other techniques [2-6]. This paper is organized as follows:- Section II describes the system under study. Section III shows the effect of the decaying DC component on the estimated phasor using the DFT. Sections from IV to IX describe Ferrero technique [7] and other techniques [2-6] for eliminating the DC component from the current signal. A comparative study has been carried out among the techniques in section X. The conclusions are presented in section XI.

2. System under study

Fig. 1 shows the simulated transmission system encountered in this study. The EMTP/ATP simulator [8] is used to model the system and generate fault data to test the performance of the technique suggested by Ferror et al. [7] and the other techniques [2-6]. The power angle δ between E_s and E_R is set as 10^0. The line length is 360 km and its operating voltage is 750 kV. The line parameters are: r_1 = 0.0484 Ω/km, L_1 = 1.2152 mH/km, C_1 = 0.0142 μF/km, r_0 = 0.29 Ω/km and L_0 = 3.8789 mH/km, C_0 = 0.0092 μF/km. Data for network A are R_A = 5 Ω and L_A = 0.18 H. Data for network B are R_B = 5 Ω and L_B = 0.3 H.

Fig. 2 shows the voltage signals of phase B observed at the sending end busbar for three line to ground faults occurring at 80 km, 180 km, 360 km respectively (measured from the sending end busbar). Fig. 3 shows the current signals of phase B observed at the sending end busbar for the same three line to ground faults and at the same fault locations of the voltage signals. It is noted from fig. 3 that the decaying DC components are presented in the current signals. It is noted also from fig. 2 and fig. 3 that the harmonic contents for the voltage and current signals are higher for faults occurring at 360 km than those occurring at 80 and 180 km. Some techniques for eliminating the decaying DC from the current signals are affected by the harmonic contents presented in the signals. The main goal of this paper is to study the effect of harmonic contents presented in the signals on the techniques of eliminating the decaying DC component. The three line to ground fault is used in this study to test the decaying DC elimination techniques. The peak values of the voltage signals are equal in magnitude for the three phases and also the peak values of the current signals are equal in magnitude (steady state values) for this type of fault (balanced fault). It is enough to test the techniques using the sampled values of the voltage and current signals of one selected phase and the results of testing the other phases are similar to those of the selected phase. Sampled values of voltage and current signals of phase B are used in this study to test the techniques.

Fig. 1. System under study.

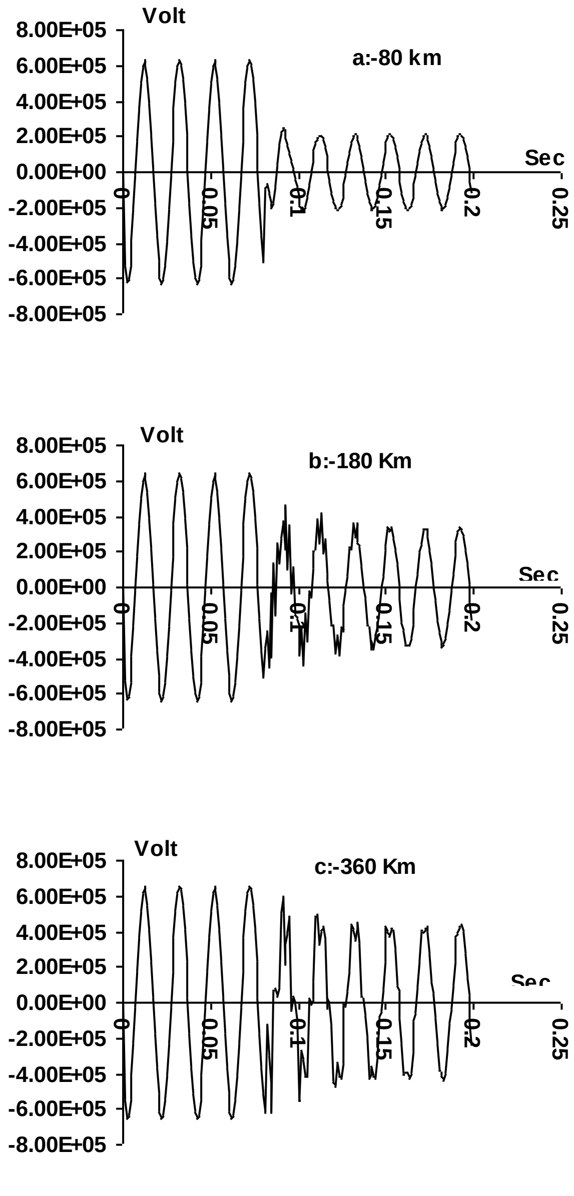

Fig. 2. The voltage signals of phase B observed at the sending end busbar for three line to ground fault.

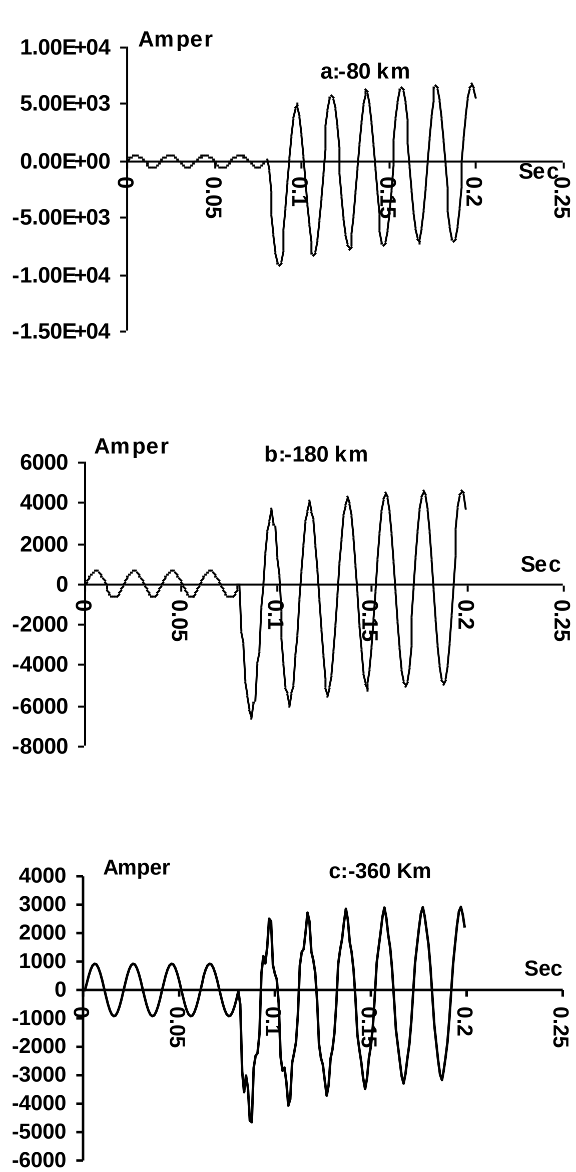

Fig. 3. The current signals of phase B observed at the sending end busbar for three line to ground fault.

3. Effect of the decaying DC component on the discrete fourier transform based phasor estimation

The input current signal to a protective device during a fault condition is assumed to include a fundamental frequency component, harmonics (up to p th order) as well as a full decaying DC offset and is given by:

$$i(t) = I_0 e^{-t/\tau} + \sum_{k=1}^{p} I_k \sin(k\omega_1 t + \theta_k)\,, \qquad (1)$$

where:- I_0 is the magnitude of the decaying DC offset, τ is the time constant of the decaying DC, I_k is the magnitude of the k th harmonic, ω_1 is the fundamental angular frequency, θ_k is the phase angle of the k th harmonic and p is the highest harmonic order in the signal.

Components with frequencies higher than the p th harmonic are assumed to be eliminated by the anti-aliasing low-pass filter.

The analog signal is converted into a digital discrete signal by an A/D conversion system:

$$i(n) = I_0 e^{-n\Delta T/\tau} + \sum_{k=1}^{p} I_k \sin(k\omega_1 n\Delta T + \theta_k)\,, \qquad (2)$$

where:- ΔT is the sampling interval and n is the n th sample.

The output of the fundamental frequency algorithm is given as [1]:

$$\hat{I}_1 = \frac{2}{M}\sum_{n=0}^{M-1} i(n) * \sin(\omega_1 n\Delta T + J\cos\omega_1 n\Delta T)\,. \qquad (3)$$

$$\hat{I}_1 = \frac{2}{M}\sum_{n=0}^{M-1} i(n) \times j \times e^{-j\omega_1 n\Delta T}\,. \qquad (4)$$

$M=N$: is the for full cycle discrete fourier transform filter, and
$M=0.5\,N$: is the for half cycle discrete fourier transform filter,

where $\hat{I}_1$ is the output of the fundamental filter corresponding to the total input signal and N is the number of samples per cycle.

It is well known that the harmonics will be eliminated by the fundamental frequency FCDFT (HCDFT filter eliminates only odd harmonics). Only the fundamental frequency and decaying DC components will show up at the output.

Fig. 4 and 5 show the effect of the decaying DC components on the estimated phasor magnitudes. Oscillations are observed in the estimated values of phasor magnitudes as shown in fig. 4. The amplitudes of these oscillations are increased if the HCDFT filter is used as shown in fig. 5. These oscillations are the results of the decaying DC components presented in the current signals. The decaying DC components should be eliminated or reduced to eliminate or reduce the oscillations from the estimated phasors.

4. Ferrero's et al. Technique [1]

In order to identify the exponential decaying component, the fault current is supposed to be sinusoidal, with a superimposed exponential component:

$$i(t) = I_1 \sin(\omega t + \alpha) + I_0 e^{-t/\tau} . \tag{5}$$

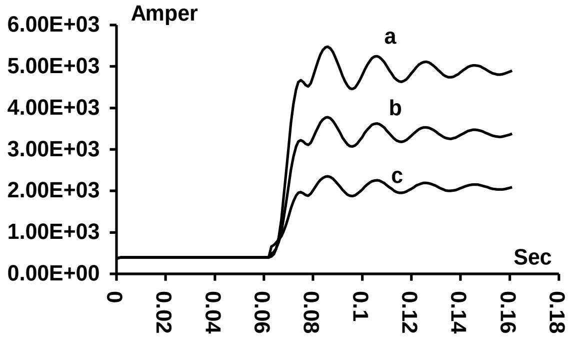

Fig. 4. The estimated current phasor magnitudes using FCDFT corresponding to current signals shown in fig. 3.

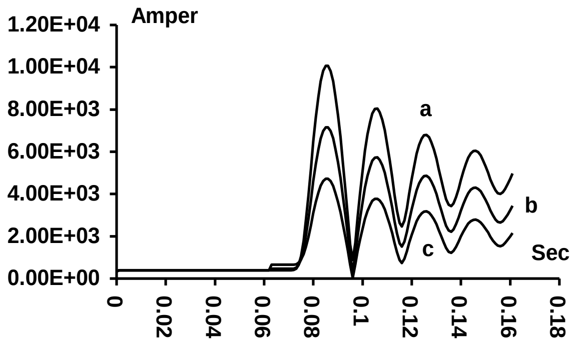

Fig. 5. The estimated current phasor magnitudes using HCDFT corresponding to current signals shown in fig. 3.

Two samples $i(t_1)$ and $i(t_1+T/2)$, $T=2\Pi/\omega$ are taken. It can be readily checked that the average value of the exponential component over the interval $(t_1+T/2,\ t_1)$ is given by

$$A_1 = [i(t_1 + T/2) + i(t_1)]/2 . \tag{6}$$

From eq. (5), it follows:-

$$A_1 = [I_0 e^{-t_1/\tau} + I_0 e^{-(t_1+T/2)/\tau}]/2 , \tag{7}$$

and hence:-

$$A_1 = [I_0 e^{-t_1/\tau} [1 + e^{-T/2/\tau}]]/2 . \tag{8}$$

Similarly, if two other samples $i(t_2)$ and $i(t_2+T/2)$ are taken, the average value of the exponential component over the interval $(t_2+T/2),\ t_2$ is given by:

$$A_2 = [I_0 e^{-t_2/\tau} [1 + e^{-T/2/\tau}]]/2 . \tag{9}$$

The ratio:-

$$\frac{A_1}{A_2} = \frac{e^{-t_1/\tau}}{e^{-t_2/\tau}} , \tag{10}$$

leads to the determination of the time constant τ as:

$$\tau = \frac{t_2 - t_1}{\ln(\frac{A_1}{A_2})} , \tag{11}$$

where t_2-t_1 can be as short as one sampling period.

From eqs. (8 and 11), the amplitude of the exponential decaying components is given by:

$$I_0 = \frac{2A_1}{e^{-t_1/\tau} [1 + e^{-T/2/\tau}]} . \tag{12}$$

Eqs. (11 and 12) allow to evaluate the amplitude and time constant of the exponential decaying component of the fault current.

Having determined these two values, each sample of the fault current can be modified by subtracting the corresponding value of the exponential component, so that the component can be completely removed.

5. Benmoual's technique [2]

A digital mimic filter was defined in ref. [2] to remove the decaying DC component from the current signal. The mimic circuit is a resistance in series with an inductance or impedance of the form

$$K(1+s\tau_1)\,, \tag{13}$$

then the exponentially decaying component at the filter output will vanish, provided its time constant is equal to τ_1 (as proven in [2]). In this equation, τ_1 is expressed in number of samples.

The sum of a gain and a differentiator circuit is represented by eq. 13. The differentiator circuit, represented in the Laplace transform *S*, can be emulated digitally by the following FIR filter:

$$1-Z^{-1}. \tag{14}$$

Introducing eqs. (14 into 13), we eventually obtain

$$K[(1+\tau_1)-\tau_1 Z^{-1}]. \tag{15}$$

Here the gain *K* has to be set in such a way that, at rated frequency, the filter gain will be 1. At 50 *Hz*, the gain is given by the following expression:

$$Gain(50Hz)=\left|K[(1+\tau_1)-\tau_1 e^{-j\omega\Delta T}]\right|=1\,. \tag{16}$$

Solving this equation for *K*, we obtain

$$K^2=\frac{1}{[(1+\tau_1)-\tau_1 * \cos\,(\frac{2*\pi*50}{Fsamp})]^2+[\tau_1 * \sin\,(\frac{2*\pi*50}{Fsamp})]^2}\,, \tag{17}$$

where Fsamp is the sampling frequency.

6. Yang's et al. technique [3]

A DFT-based decaying dc offset removal scheme that accurately estimates the phasor from a fault current has been proposed [3]. The main components of a fault current signal can be expressed by

$$i(t)=I_1\cos(\omega_1 t+\phi_1)+I_0\exp(-\alpha * t)\ , \tag{18}$$

where

$$1/\alpha=\tau$$

The signal is sampled with *N* samples per cycle to produce the sample set

$$i(n)=I_1\cos(\omega_1 n/50N+\phi_1)+I_0\exp(-\alpha * n/50N)\,, \tag{19}$$

n = 0,1,2,..., N-1

The fundamental component calculated using the DFT filter is given by

$$\hat{I}(r)=\frac{2}{M}\sum_{n=0}^{M-1} i(n+r)e^{-Jn\theta}\ , \tag{20}$$

where

$$\theta=\frac{2\pi}{N}\,;$$

M=N for FCDFT;
M=0.5 N for HCDFT;
r denotes the index of the moving data window.

Combining eqs. (19 and 20), the fundamental phasor is expressed as

$$\hat{I}(r)=A_r+B_r\,, \tag{21}$$

where

$$A_r=I_1 e^{J\phi_1}e^{jr\theta}\,. \tag{22}$$

$$B_r=\frac{2}{M}I_0 e^{-\alpha r/50N}\sum_{n=0}^{M-1} e^{-\alpha n/50N}e^{jn\theta}\,. \tag{23}$$

Since the conventional DFT filter does not take the decaying DC offset into consideration it incurs errors in estimating the phasor when the decaying DC offset is presented in a fault signal. If we want to get the exact solution, we must take B_r into consideration. Thus, we define

$$a = e^{j2\pi/N} = e^{j\theta} \ , \ d = e^{-\alpha/50N} . \quad (24)$$

After some algebraic manipulation, it yields

$$d = \frac{\hat{I}(r+2) - a\hat{I}(r+1)}{\hat{I}(r+1) - a\hat{I}(r)} . \quad (25)$$

$$A_r = \frac{\hat{I}(r+1) - d\hat{I}(r)}{(a-d)} . \quad (26)$$

Then, the accurate fundamental current phasor can be obtained as

$$I_1 = abs(A_r) . \quad (27)$$

$$\phi_1 = angle(A_r e^{-j2\pi(r-1)/N}) . \quad (28)$$

Thus, from (25-28), we can remove the decaying DC offset from the fault current signal using the term "d". The phasor is accurately computed from the three consecutive DFT estimates $\hat{I}(r), \hat{I}(r+1)$, and $\hat{I}(r+2)$ by using recursive computing and so the technique is suitable for real time implementation.

7. Sidhu's et al. technique [4]

Two FCDFT filters are used to eliminate the DC component by this technique. One tuned at the fundamental frequency and the other at the m th harmonic. The harmonics are eliminated by the fundamental frequency FCDFT filter. Only the fundamental frequency and decaying DC components will show up at the output. Since accurate phasors of the fundamental components are desired, the elimination of the contamination of the decaying DC offset in the fundamental frequency FCDFT output is required. The first step towards achieving this objective is to find the response of the fundamental frequency FCDFT only to the decaying DC offset ($I_0 \, e^{-nT/\tau}$). This response is defined in (29)

$$\hat{I}_1^{dc} = \frac{2}{N} \times jI_0 \frac{1 - e^{-N\Delta T/\tau}}{1 - e^{-\Delta T/\tau} e^{-j\omega_1 \Delta T}} , \quad (29)$$

where $\hat{I}_1^{dc}$ is the output of the fundamental frequency FCDFT solely corresponding to a decaying DC offset and N is the number of samples per cycle.

The output of the fundamental frequency FCDFT due to fundamental component can be extracted using eq. (30)

$$\hat{I}_1^{f} = \hat{I}_1 - \hat{I}_1^{dc} , \quad (30)$$

where $\hat{I}_1^{f}$ is the output of the fundamental frequency FCDFT corresponding to the fundamental component of the input signal.

Using eq. (30), phasors of the fundamental components can be estimated provided that the fundamental frequency FCDFT response due to the decaying DC offset can be determined. The response of the fundamental frequency FCDFT due to the decaying DC offset is determined once the parameters of the decaying DC offset are found. These parameters can be determined from the output of the m th harmonic filter.

The frequency of the m th harmonic should be above the cut-off frequency of the low-pass filter and below one-half of the sampling frequency. The output of the m th harmonic FCDFT filter will solely include the effect of the decaying DC component and is given as follows:

$$\hat{I}_m^{dc} = \frac{2}{N} \times jI_0 \frac{1 - e^{-N\Delta T/\tau}}{1 - e^{-\Delta T/\tau} e^{-j\omega_1 m\Delta T}} . \quad (31)$$

For simplicity, the expression $e^{-N\Delta T/\tau}$ is denoted as E. It was shown in ref. [4] that the parameters of the decaying DC offset can be determined from the following equations:-

$$E = \frac{R}{R\cos(\omega_1 m\Delta T) + I\sin(\omega_1 m\Delta T)} . \quad (32)$$

$$\frac{2}{N} I_0 (1 - E^N) = \frac{R(1 + E^2 - 2E\cos(\omega_1 m \Delta T)}{E\sin(\omega_1 m \Delta T)} . \quad (33)$$

The values of E and $(2/N)$ $I_0(1\text{-}E^N)$ can be obtained from eqs. (32 and 33) as real R and imaginary (I) output of the m th harmonic FCDFT, and the values of $\cos(\omega_1 m\Delta T)$ and $\sin(\omega_1 m\Delta T)$ are known. The output of the fundamental FCDFT corresponding to the decaying DC offset, $\hat{I}_1^{dc}$, can be determined using these values (i.e. E and $(2/N)$ $I_0(1\text{-}E^N)$) by substituting in eq. (29). Therefore the fundamental component phasor of the input signal can be determined using eq. (30).

8. Shan's technique [5]

Shan derived a mathematical expression for the error resulting from estimating a phasor with the DFT. The source of this error is the decaying DC component presented in the signal used in estimating the phasor. The error is defined as:-

$$\psi(M+1) = \frac{[I_r(M+1) - I_r(M)] + j[I_i(M+1) - I_i(M)]}{(Ee^{-j(2\pi/N)} - 1)} . \quad (34)$$

M=N for FCDFT, M=0.5N for HCDFT

where I_r and I_i are the real and imaginary parts of the fundamental phasor estimated by the DFT. E is equal to $e^{-N\Delta T/\tau}$.

The accurate real part and imaginary part of the fundamental phasor can be calculated as follows:-
The accurate real part of the phasor is:-

$$I_r(M) - \mathrm{Real}(\psi(M+1)). \quad (35)$$

The accurate imaginary part of the phasor is:-

$$I_i(M) - \mathrm{Imag}(\psi(M+1)). \quad (36)$$

Therefore, the accurate fundamental phasor can be obtained by two sequential phasors and simple computation in eqs. (35 and 36). The total amount of data used for obtaining the results of eqs. (34-36) are one cycle plus one sample for FCDFT and half cycle plus one sample for HCDFT.

9. Guo's et al. technique [6]

Guo et al. used two partial sums to estimate the parameters of the decaying DC component presented in the current signal. The first is the sum of the odd number samples taken from complete cycle of the fundamental frequency of the current signal. This sum is defined as:-

$$PS_1 = i(1) + i(3) + \cdots + i(N-1) . \quad (37)$$

It was shown in ref. [6] that PS_1 yields:-

$$PS_1 = I_0 \frac{E(E^N - 1)}{E^2 - 1} . \quad (38)$$

The second is the sum of the even number samples taken from a complete cycle of the current signal. This sum is defined as:-

$$PS_2 = i(2) + i(4) + \cdots + i(N) . \quad (39)$$

It was shown in ref. [6] that PS_2 yields:-

$$PS_2 = I_0 \frac{E^2(E^N - 1)}{E^2 - 1} . \quad (40)$$

From eqs. (38 and 40), we can solve the E and I_0 as follows:-

$$E = \frac{PS_2}{PS_1} . \quad (41)$$

$$I_0 = \frac{E^2 - 1}{E(E^N - 1)} PS_1 . \quad (42)$$

Once E and I_0 are obtained, the set of sampled values can be modified as

$$i(k\_new) = i(k) - I_0 E^k, k = 0,1,\cdots,N . \quad (43)$$

This new set of sampled values no longer contains the exponentially decaying component. Applying the Fourier algorithm to this new set of samples, we can accurately extract the i-th harmonic component.

10. A comparative study

The six techniques for eliminating the decaying DC component [2-7] are compared using half and full cycle discrete Fourier transform filters. The voltage and current waveforms shown in figs. 2 and 3 are used in the comparative study. The Matlab software package [9] is used to simulate the techniques. The performance index suggested by Shan [5] is used in this study to compare the results obtained from the techniques.

10.1. Comparing the techniques using the half cycle discrete Fourier transform filter

The six techniques are compared using the half cycle discrete Fourier transform filter and the simulation results are shown in figs. 6 and 7. The following remarks are obtained from these results:-

1. The current phasor magnitudes and the apparent impedances are correctly estimated using Ferrero's et al. technique [7] as shown in figs. 6-a and 7-a.
2. The current phasor magnitude and the apparent impedance are correctly estimated using Benmoual's technique [2] at 80 km fault location. But when this technique is used for estimating the current phasor magnitudes and the apparent impedances at 180 km and 360 km, the deviation between the calculated and true values are large as shown in figs. 6-b and 7-b.
3. The current phasor magnitudes and the apparent impedances are correctly estimated using Yang, Sidhu, Shan, and Guo [3-6] techniques at 80 km fault location. But when these techniques are used for estimating the current phasor magnitudes and the apparent impedances at 180 km and 360 km, oscillations are observed in the estimated values as shown in figs. 6 and 7.
4. The estimated values of the current phasor magnitude using Ferrero's [7] technique [7] are more accurate and converged faster to the desired values than the other techniques[2-6] since it needs a half cycle and a sample to eliminate the decaying DC component as shown in fig. 10-a.

10. 2. Comparing the techniques using the full cycle discrete Fourier transform filter

The six techniques are compared using the full cycle discrete Fourier transform filter and the simulation results are shown in figs. 8 and 9. The following remarks are obtained from these results:-

1. The current phasor magnitudes and the apparent impedances are correctly estimated using Ferrero's et al. technique [7] as shown in figs. 8-a and 9-a. It is noted from these figs. that the maximum overshoots observed in the estimated current phasor magnitudes are lower than those shown in fig. 6-a.
2. The current phasor magnitude and the apparent impedance are correctly estimated using Benmoual's technique [2] at 80 km fault location. But when this technique is used for estimating the current phasor magnitudes and the apparent impedances at 180 km and 360 km, the deviation between the calculated and true values are large as shown in figs. 8-b and 9-b. The estimated using this technique are the same whether the filter used is half or full cycle discrete Fourier transform.
3. The current phasor magnitudes and the apparent impedances are correctly estimated using Yang, Sidhu, Shan, and Guo [3-6] techniques at 80 km fault location. But when these techniques are used for estimating the current phasor magnitudes and the apparent impedances at 180 km and 360 km, oscillations are observed in the estimated values as shown in figs. 8 and 9. The amplitudes of these oscillations are smaller than those shown in figs. 6 and 7.
4. The estimated values of the current phasor magnitude using Ferrero's [7] technique [7] are more accurate and converged faster to the desired values than the other techniques [2-6] since it needs a half cycle and a sample to eliminate the decaying DC component as shown in fig. 10-b.

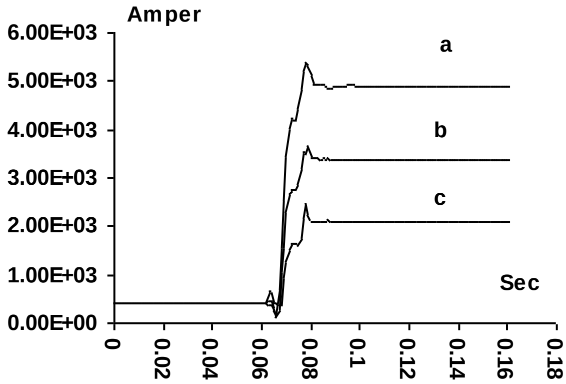

(a) Ferrero's et al. technique [7]

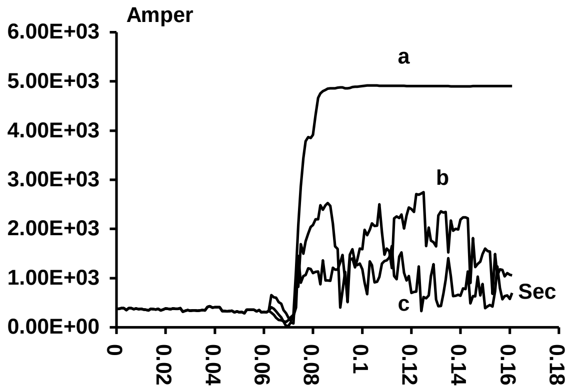

(b) Benmoual's technique [2]

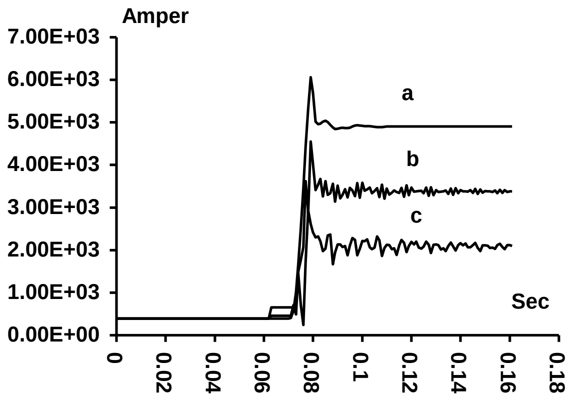

(c) Yang's et al. technique[3]

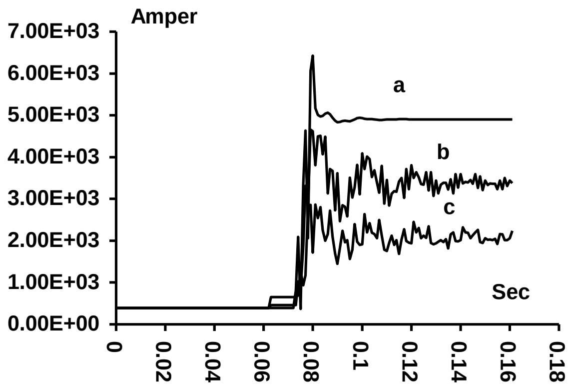

(d) Sidhu's et al. technique[4]

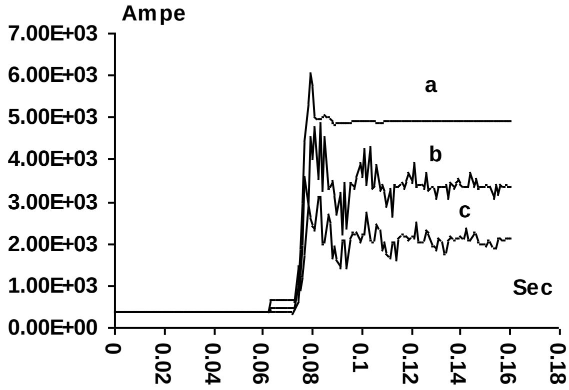

(e) Shan's technique [5]

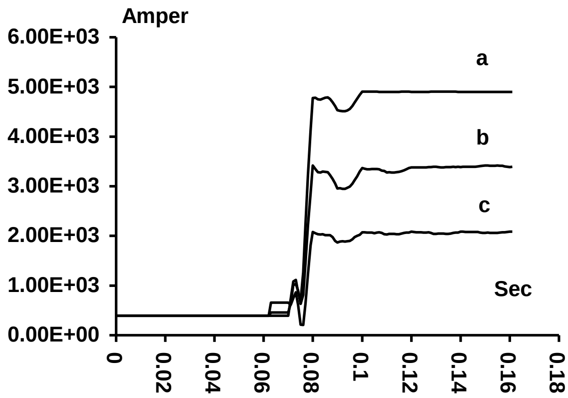

(f) Guo's et al. technique[6]

Fig. 6. The estimated current phasor magnitudes using HCDFT.

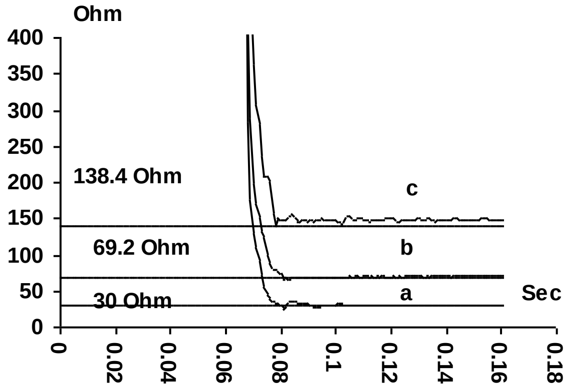

(a) Ferrero's et al. technique [7]

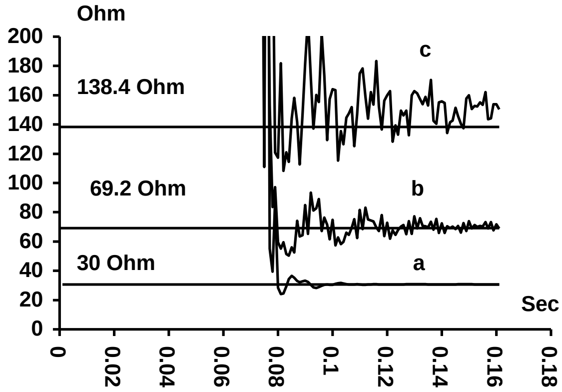

(d) Sidhu's et al. technique[4]

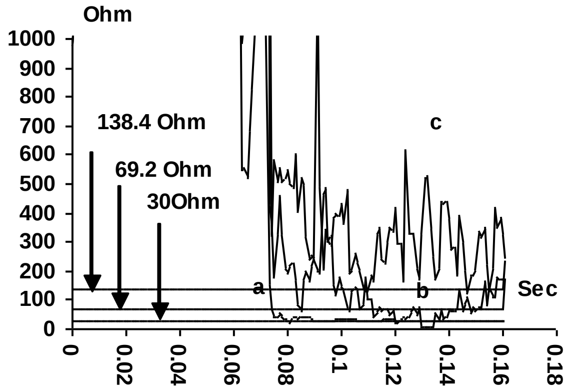

(b) Benmoual's technique [2]

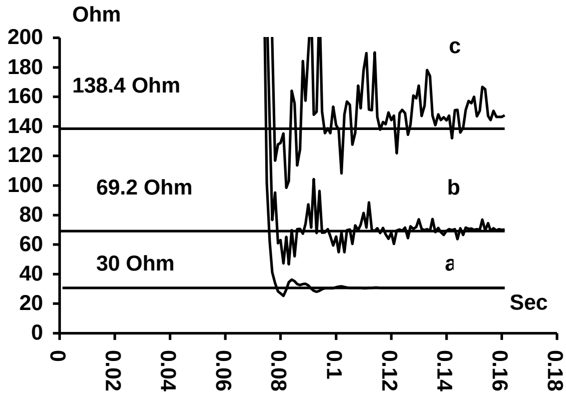

(e) Shan's technique [5]

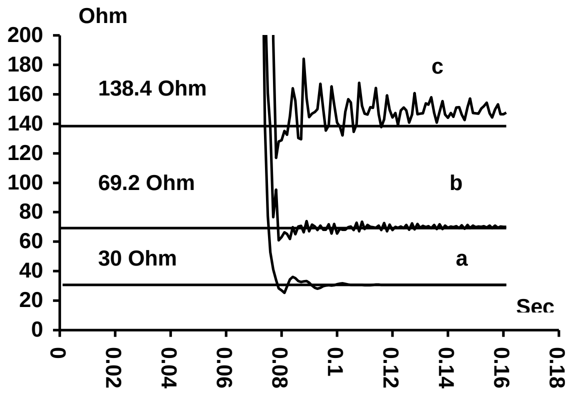

(c) Yang's et al. technique[3]

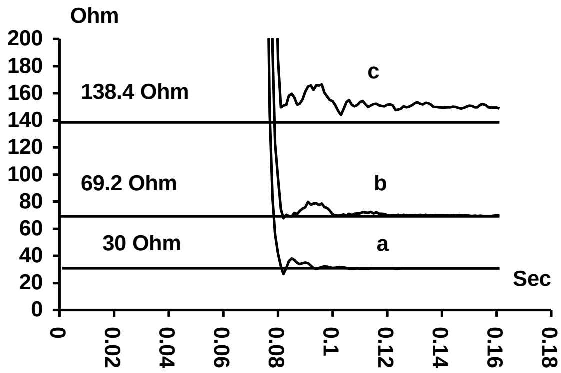

(f) Guo's et al. technique[6]

Fig. 7. The estimated apparent impedance using HCDFT.

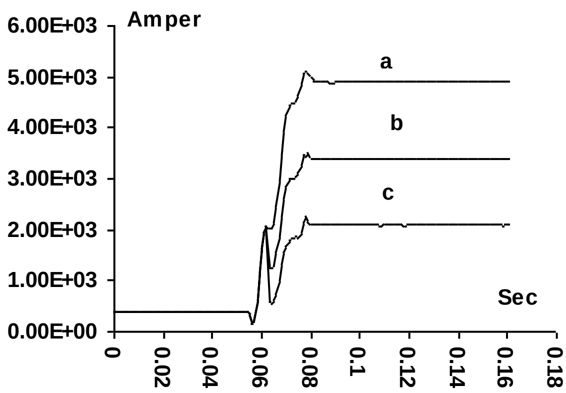

(a) Ferrero's et al. technique [7]

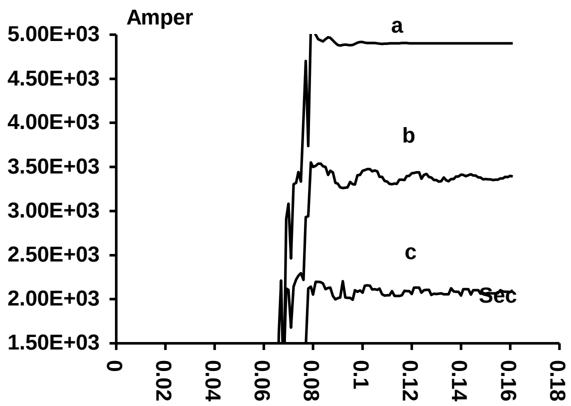

(d) Sidhu's et al. technique[4]

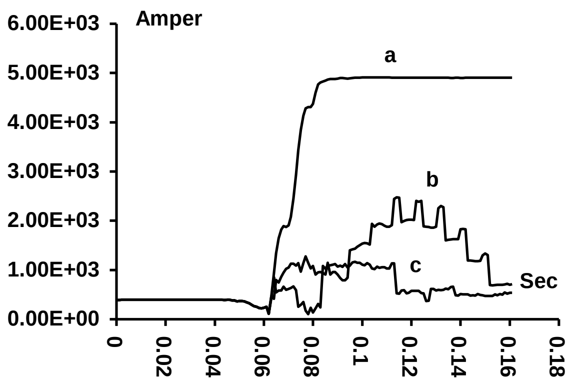

(b) Benmoual's technique [2]

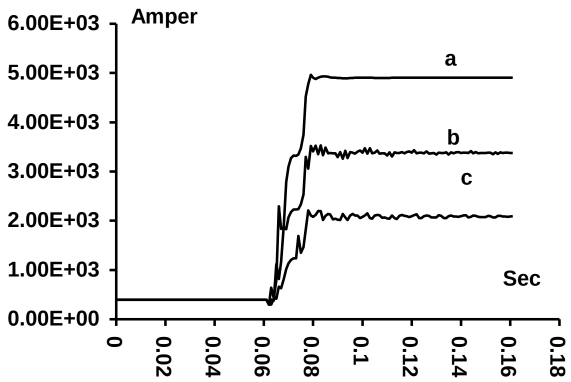

(e) Shan's technique [5]

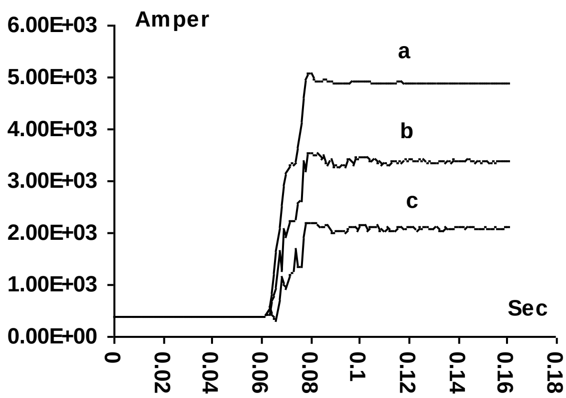

(c) Yang's et al. technique[3]

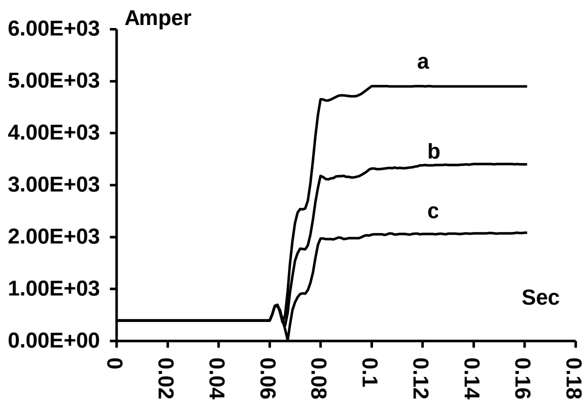

(f) Guo's et al. technique[6]

Fig. 8. The estimated current phasor magnitudes using FCDFT.

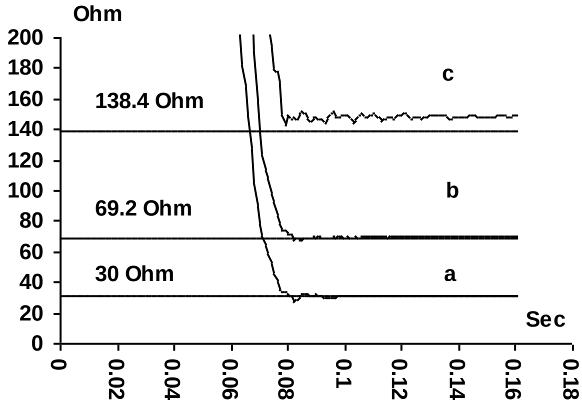

(a) Ferrero's et al. technique [7]

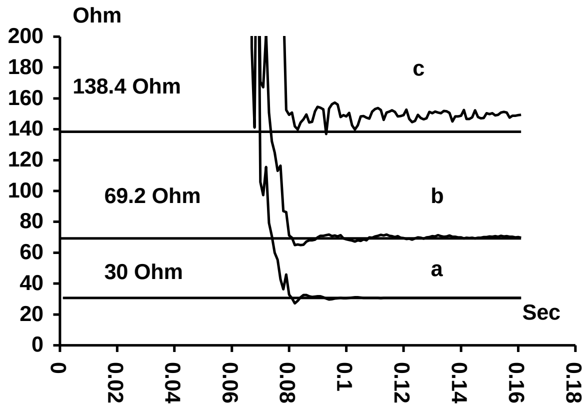

(d) Sidhu's et al. technique[4]

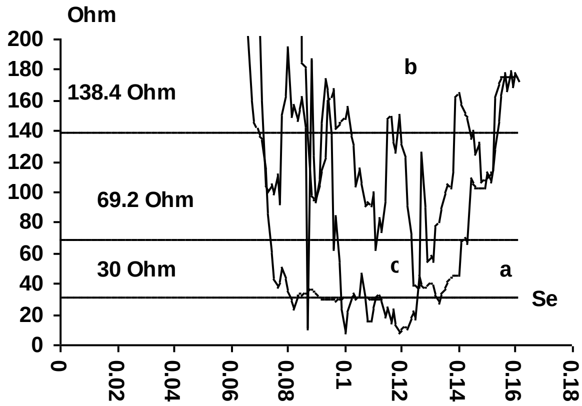

(b) Benmoual's technique [2]

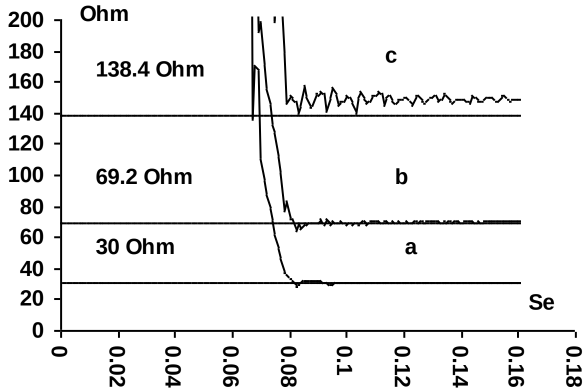

(e) Shan's technique [5]

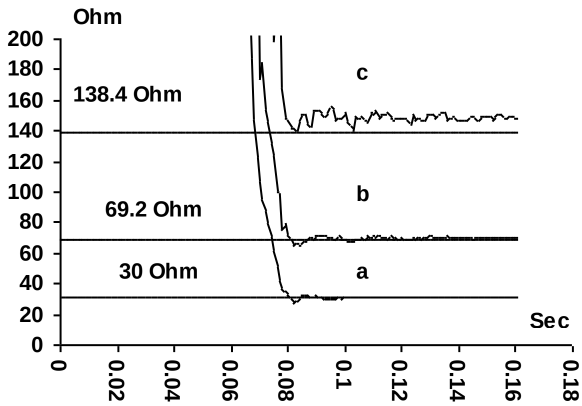

(c) Yang's et al. technique[3]

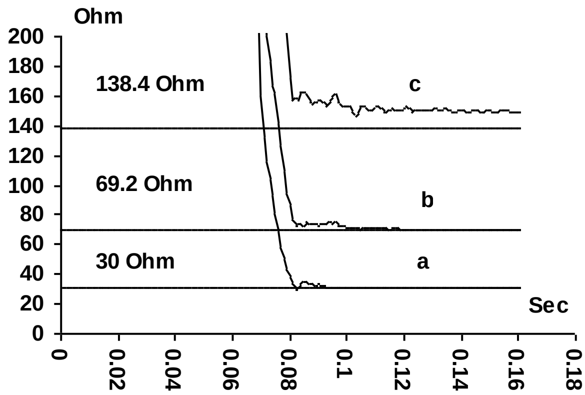

(f) Guo's et al. technique[6]

Fig. 9. The estimated apparent impedance using FCDFT.

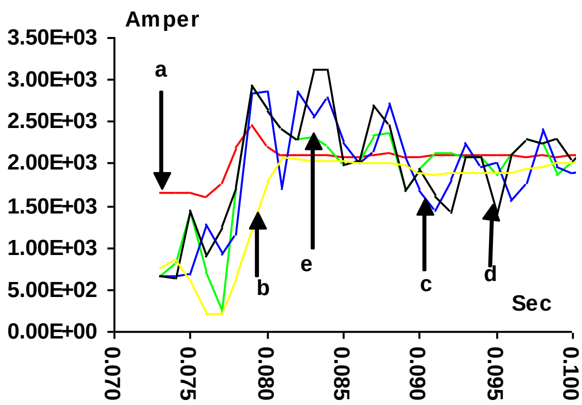

(a) Using HCDFT

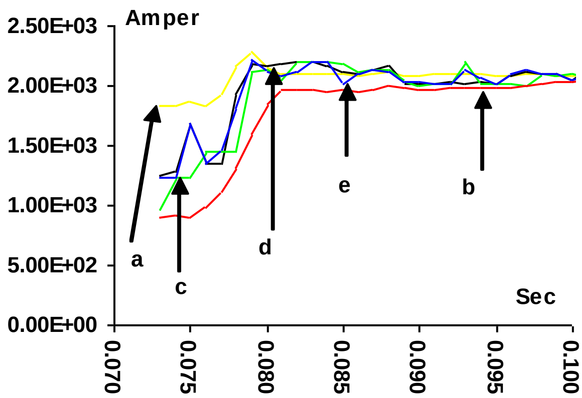

(b) Using FCDFT

Fig. 10. The estimated current phasor magnitude at 360 km
(a) Ferrero (b) Guo (c) Sidhu (d) Shan (e) Yang.

10. 3. Performance index evaluation

The performance index suggested by Shan [5] is used in this study to compare the results obtained from the techniques. This performance index is the Percentage Root-Mean-Square Error (*PRMSE*) and is defined as:-

$$PRMSE = \frac{\sqrt{\sum_{k=n}^{n+N-1}(kth filter output - steady\ state value)^2 / N}}{steady\ state value} \times 100\% \cdot \quad (44)$$

This performance index is used to evaluate the overall filtering performance. Since the estimated phasor is calculated at the beginning of the fault period using pre-fault and post-fault samples, the beginning index n is the sample at one cycle after fault to avoid using pre-fault samples.

The results are shown in tables 1, 2, and 3 for 80 km, 180 km, and 360 km fault location respectively. Obviously the Ferrero's et al. [7] technique has the best performance.

Table 1
Performance evaluation results for 80 Km fault location

	Prmse	
Algorithms	Hcdft	Fcdft
Ferrero	1.377E-3	6.318E-4
Benmoual	4.327E-3	1.921E-3
Yang	4.804E-3	2.086E-3
Sidhu	6.288E-3	2.591E-3
Shan	4.805E-3	1.0775E-3
Guo	2.733E-1	2.250E-2

Table 2
Performance evaluation results for 180 Km fault location

	Prmse	
Algorithms	Hcdft	Fcdft
Ferrero	1.047E-3	8.322E-4
Benmoual	3.383E-1	2.733E-1
Yang	3.543E-2	1.963E-2
Sidhu	1.396E-1	2.318E-2
Shan	1.494E-1	1.627E-2
Guo	6.9089E-2	3.734E-2

Table 3
Performance evaluation results for 360 Km fault location

	Prmse	
Algorithms	Hcdft	Fcdft
Ferrero	5.662E-3	4.122E-3
Benmoual	3.394E-1	8.966E-1
Yang	6.245E-2	2.262E-2
Sidhu	1.458E-1	2.777E-2
Shan	1.504E-1	1.967E-2
Guo	7.979E-2	3.873E-2

11. Conclusions

The technique suggested by Ferrero et al. [7] is used in this paper to study the effect of eliminating the decaying DC component from the current signal on the discrete Fourier transform based phasor estimation. This technique is compared with other techniques for eliminating the decaying DC component [2-6]. The voltage and current waveforms are generated using the Alternative Transient Program (ATP) [8] to test the techniques. The techniques are simulated using the Matlab software package [9]. The performance index suggested by Shan [5] is used to compare the techniques. The estimated values of Ferrero's et al. technique are close to the desired values and converged faster than other techniques. Ferrero's et al. technique has also the best performance index.

References

[1] A. Phadke, J. Thorp and M. Adamiak, "A New Measurement Technique for Tracking Voltage Phasor, Local System Frequency", IEEE Transactions on Power Apparatus and Systems, Vol. PAS-102 (5), pp. 1025-1038, May (1983).

[2] G. Benmouyal, "Removal of DC-Offset in Current Waveforms Using Digital Mimic Filtering", IEEE Transactions on Power Delivery, Vol. 10 (2), pp. 621-630, April (1995).

[3] J. Yang and C. Liu, "Complete Elimination of DC Offset in Current Signals for Relaying Applications", in Proc. IEEE Power Engineering Society Winter Meeting, Vol. 3, pp. 1933-1938 (2000).

[4] T. Sidhu, X. Zhang, F. Albas and M. Sachdev, "Discrete-Fourier-Transform-Based Technique for Removal of Decaying DC Offset from Phasor Estimates", Proc. Inst. Elect. Eng. Generation, Transmission Distribution, Vol. 150 (6), pp. 745-752, Nov. (2003).

[5] C. Shan, "A Discrete Fourier transform Based Adaptive Mimic Phasor Estimator for Distance Relaying Applications", IEEE Transactions on Power Delivery, Vol. 21 (4), pp. 1836-1846, October (2006).

[6] Y. Guo, M. Kezunovic and D. Chen, "Simplified Algorithms for Removal of the Effect of Exponentially Decaying DC-Offset on Fourier Algorithm", IEEE Transactions on Power Delivery, Vol. 18 (3), pp. 711-717, July (2003).

[7] A. Ferrero, S. Sangiovanni and E. Zappitelli, "A Fuzzy-Set Approach to Fault-Type Identification in Digital Relaying", IEEE Transactions on Power Delivery, Vol. 10 (1), January (1995).

[8] Alternative Transient Program Rule Book, Jul., Leuven EMTP Center (1987).

[9] A. Cavallo, R. Setola and F. Vasco, Using Matlab, Simulink and Control System Toolbox, Printice Hall (1994).

Received September 3, 2007
Accepted November 29, 2007